Intelligent Transportation and Smart Cities
V. Mezhuyev et al. (Eds.)

doi:10.3233/ATDE240391

Study on Axial Compression Performance of Ribbed Thin-Walled Square Steel Tube Recycled Concrete Short Column

Zhiming LI[1], Jinsong LEI and Xianzao WU
School of Civil Engineering and Architecture, Southwest University of Science and Technology, Mianyang City, Sichuan Province, China

Abstract. Driven by the new infrastructure of smart city, in order to explore the sustainable development of smart city, this paper starts from the reuse of waste concrete, and studies the mechanical properties of recycled concrete short columns of ribbed thin-walled square steel tube, taking the number of stiffeners and the ratio of height to thickness of stiffeners as parameters. Two types of square steel tube recycled concrete short columns were designed: one with ribs and the other with ribs. The final load capacity and failure mode of ribbed square steel tube recycled concrete short columns were primarily investigated. The mechanical properties of double-ribbed, single-ribbed and non-ribbed square steel tube recycled concrete axial compression short columns were analyzed from the load-displacement relationship. The test results show that the setting of stiffening ribs not only improves the bearing capacity of the specimen, but also effectively slows down the local buckling of the steel pipe. When the width-to-thickness ratio of the specimen is small, increasing the number of stiffeners has little effect on the bearing capacity when the steel ratio remains unchanged. With the increase of the height-thickness ratio of the stiffener, the bearing capacity of the specimen and the stability of the tube wall have an increasing trend. On this basis, the finite element software ABAQUS was used to establish the analysis model. The analysis's findings demonstrate that the finite element model's failure mode and load-displacement curve mostly agree with the findings of the experiments.

Keywords. Thin-walled ribbed square steel tube, recycled concrete, static test, finite element simulation

1. Introduction

With Given the building industry's rapid development in China, many buildings have produced a lot of energy consumption and waste of resources in the construction process, resulting in more and more serious environmental problems. According to statistics, China's annual construction industry generated by the construction waste up to 90 million tons, of which concrete accounted for 35%[1]. After the waste concrete is treated, the obtained aggregate is re-allocated into repurposed concrete, which can not only reduce the pollution of discarded concrete to the environment, but also promote the construction of smart cities. The construction of smart city can not only raise the quality and effectiveness of urban governance, but also improve the quality of life of

[1] Corresponding Author: Zhiming LI, 2622699128@qq.com

residents. Numerous academics both domestically and internationally have researched the development of smart cities. Robert[2]pointed out that smart city is the foundation of sustainable urban development. Laura[3]proposed the main characteristics of green building building literacy, through better construction, operation and maintenance to reduce construction waste. Spicer[4] used the unique survey data of residents to study smart city technology. Nilssen[5] developed a typology of smart city initiatives based on the existing literature on smart cities. Manirathinam[6] used the APPRESAL method to evaluate the performance and satisfaction of sustainable clean energy transport in cities. This paper studies the reuse of waste concrete to explore the road of sustainable development of smart cities.

Scholars from both domestic and international universities are currently conducting theoretical analysis and experimental study on recycled concrete. Short steel tube columns filled with self-compacting alkali-activated slag concrete were the subject of experimental and numerical research by Shivam Kumar[7]. The influence of Erhan[8] on the geometrical and material properties of RACFST columns was studied. Xiao Jianzhuang[9,10]verified the possibility of using recycled concrete instead of ordinary concrete through a large number of experiments. Wang[11]carried out a long-term deformation test of steel tube expansion recycled concrete members. Huang[12] designed four square steel tube recycled concrete short columns to study their cross-section forms. However, there are few studies on ribbed steel tube recycled concrete, especially on ribbed square steel tube recycled concrete. Therefore, in this paper, four ribbed square steel tube recycled concrete short columns and one unribbed square steel tube recycled concrete short column are selected for experimental research with the number of stiffeners and the stiffeners' height-thickness ratio as the main parameters, and the ultimate bearing capacity of ribbed square steel tube recycled concrete short columns and the influence of various parameters on the mechanical performance are analyzed. At the same time, ABAQUS established the finite element model for theoretical analysis.

2. Test Overview

2.1. Specimen Design and Production

A total of five square steel tube recycled concrete short column specimens were designed, including one non-ribbed, three single-ribbed and one double-ribbed specimen. The specimens' width-to-thickness ratio is 80, and every specimen's height is three times its width, that is, L/B = 3. Table 1 shows the major information for every sample.

Table 1. Specimen details

numbering	B×t×L/mm	h_s×t_s/mm	h_s/t_s	α	$f_s f_s'$/MPa	N_u/k	N_0/kN	N_u/N_0	remark
SU-0-0	160×2×480	—	—	0.0526	235	914	919	0.994	apleuria
SS-1-20	160×2×480	20×2	10	0.0596	235	1010	1053	0.959	single rib
SS-1-30	160×2×480	30×2	15	0.0631	235	1128	1160	0.972	single rib
SS-1-40	160×2×480	40×2	20	0.0667	235	1145	1176	0.974	single rib
SS-2-20	160×2×480	20×2	10	0.0667	235	1129	1156	0.976	double rib

Annotation:SS represents the stiffened repurposed concrete column made of square steel tubes, SU represents the unstiffened repurposed concrete column made of square steel tubes ; the first number after the letters SU and SS denotes the number of stiffeners, and the second number denotes the height of stiffeners. h_s and t_s are the height and thickness of the stiffener, respectively ;The square steel tube's side length, wall thickness, and height are denoted as B, t, and L, correspondingly. α denotes the section's steel ratio ; f_s and f_s' represent the yield strength of steel tube and stiffener respectively ; N_u is The test determines the specimen's ultimate bearing capability; N_0 is the maximum carrying capacity of the specimen measured by finite element simulation.

The mixing method of recycled concrete is manual mixing, which is composed of P42.5 ordinary Portland cement, coarse aggregate, ordinary natural river sand and school laboratory tap water. The mix ratio is m water: m cement: m coarse aggregate: m sand = 1:1.89:6.05:3.26., and the substitution rate of recycled aggregate is 100 %. Recycled aggregate is made of building demolition waste coagulation processing, crushing index is 16.4%. The cube compressive strength f_{cu} of recycled concrete is measured by the cube test block with a side length of 150 mm, which is poured at the same time when the test piece is poured and cured under the exact same circumstances. The cubic and axial compressive forces of recycled concrete are 39.2 MPa and 25.8 MPa, respectively.

2.2. Test Equipment and Measuring Point Arrangement

The transverse and longitudinal strain gauges are set in the middle of the middle part around the steel tubular to obtain the law of the strain of the steel tube changing with the load. Two displacement meters are symmetrically arranged at the axial foot of each specimen to accurately measure axial deformation of the specimen. The cross-sectional form of the specimen and the loading and measuring device are shown in Figure 1.

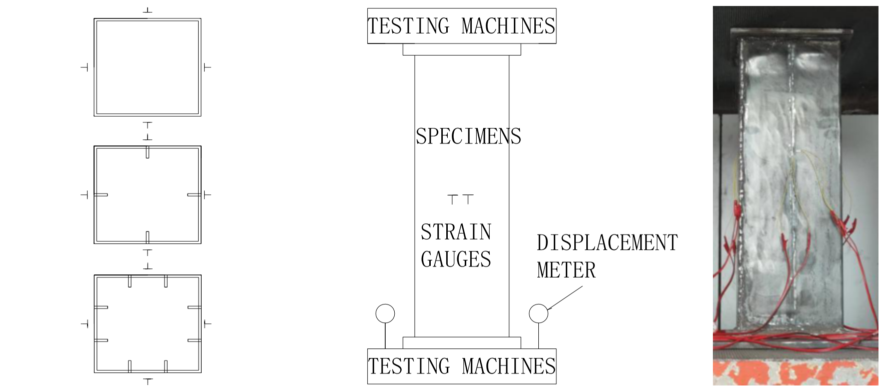

(a)Measuring point arrangement (b)Diagram of loading device (c)Test loading photos

Figure 1. Test setup and measurement points arrangement

2.3. Loading Method

At Southwest University of Science and Technology, the test is conducted at the structural laboratory. The experiment loading apparatus uses an electro-hydraulic servo long column pressure testing machine with a 1000kN QXZ-1000 microcomputer controlled system. The upper section of the device is provided with displacement loading by hydraulic jack, and the lower part is spherical hinge. The test adopts the method of load control to load step by step. Before the formal loading, check whether the equipment is working properly, and pre-load the two-stage load to reduce the space between the specimen and the testing apparatus. The entire preloaded load is not greater than 20% of the anticipated final load. When formally loaded, each stage's loading value is equal to 10% of the anticipated ultimate load, loaded to this stage's maximum load, and the loading period is two minutes. Each stage's loading value is 5% of the projected ultimate load after loading to 70% of the estimated ultimate load, and the loading period is between two and three minutes. The loading rate of the whole loading process is maintained at 0.6 kN/s. When the load of the specimen drops below 80 % of the peak load, the test has finished and the loading has paused. The pressure sensor measures the load value, the dial indication measures the axial displacement, and the DH3816N strain data acquisition device collects longitudinal and transverse strain information.

3. Experiment Results and Analysis

3.1. Failure Form of Specimen

The specimen is in full section compression at the start of the loading process, and the surface of the steel tube has not changed significantly. As the load increases, so does the specimen's cross-section distortion, resulting in local buckling of the pipe wall. At the beginning, the buckling develops slowly, accompanied by slight crackling. After the full capacity for bearing is reached, the axial deformation of the specimen continues to increase, and the development of the drum is more obvious. The sound of the separation of the steel tube wall from the concrete can be heard. Finally, the loading was stopped due to the tearing of the corner of the steel pipe. During the failure, 2-5 local wrinkling occurred on the surface of all specimens and the degree of buckling along the four surfaces was basically the same. The steel tube wall of the non-rib specimen forms a large bulge, while the steel tube wall of the stiffened rib specimen appears multiple half-wave bulges, and the bulge appears later than the non-rib specimen. This is due to the existence of the stiffener, which delays the local buckling of the steel tube and increases the flexural stiffness of the pipe wall. Figure 2 is the failure mode of each specimen.

(a) SU-0-0 (b) SS-1-20 (c) SS-1-30 (d) SS-1-40 (e) SS-2-20

Figure 2. Failure modes of specimens

3.2. Load-displacement Curve

Figure 3 depicts the load-displacement test curves for each specimen. The figure shows that when the specimen is in the elastic stage, the load-displacement curve for each specimen is approximately linear, with the load corresponding to the displacement. The elastic working stage of the ribbed specimen is obviously longer than that of the non-ribbed specimen. As the axial load continues to increase, the curve of load displacement increasingly deviates from the straight path, entering the plastic stage. Following the specimens' maximum bearing capacity, a notable decrease was observed in the load-displacement curve. The ribbed specimens exhibit superior ductility, a gentler descending section of the curve, a higher peak load, and an evident improvement in bearing capacity when compared to the non-ribbed specimens. The bearing capacity of ribbed specimens SS-1-20, SS-1-30, SS-1-40 and SS-2-20 increased by 10.51%, 23.38%, 25.3% and 23.57% respectively compared with that of non-ribbed specimens SU-0-0. It shows that the stiffening rib improves delays the local buckling of the steel pipe and the steel pipe's limiting influence on the recycled concrete.

Figure 3a gives the relationship curve of the effect of varying numbers of stiffeners on capacity for bearing at the same steel ratio. In the elastic stage, the curve slope is relatively near and the axial stiffness is basically the same. It is clear that as the number of stiffeners increases, the specimen's axial stiffness has little effect. For the short column made of reclaimed concrete and thin-walled ribbed square steel tubes, when B/t is 80, the bearing capacity does not increase with the rise of the amount of stiffening elements, but rather drops significantly. This is because increasing the number of stiffeners lowers the moment of inertia of a single stiffener, resulting in prematurely local buckling on the pipe wall and a loss in bearing capacity.

Figure 3b shows the relationship graph for the effect of various stiffener height-thickness ratios on capacity for bearing. The load-displacement curve during the elastic stage is basically coincident, indicating that the axial stiffness is not affected by the increase of the stiffener height-thickness ratio. In the elastic-plastic stage, the load-displacement curve of the specimen SS-1-30 began to deviate, but the relationship curves of the specimens SS-1-20 and SS-1-40 still roughly coincided. The stiffener's height-thickness ratio can be increased to effectively boost the specimen's final bearing capacity. The specimens SS-1-30 and SS-1-40 have a larger bearing capacity than the specimen SS-1-20, by 11.65% and 13.39%, correspondingly. However, the growth rate of bearing capacity gradually slows down as the height-thickness ratio increases. This is due to the fact that when the specimen's steel ratio rises, the recycled concrete's ability to serve as a constraint becomes less effective and the rate at which bearing capacity increases slows down. When the steel ratio of the specimen reaches a certain value, its constraint on recycled concrete reaches the maximum, and its bearing capacity also reaches the maximum.

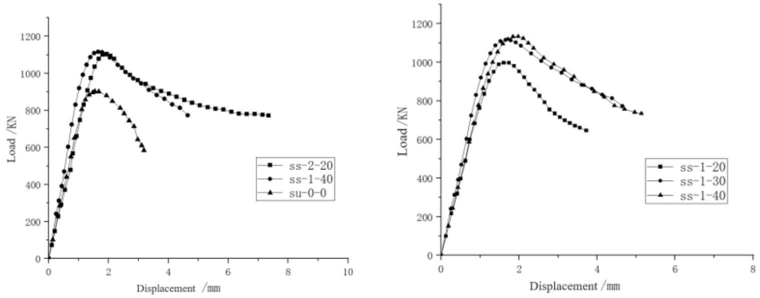

(a)Different number of stiffeners (b) Different stiffener height-thickness ratio

Figure 3. Load-displacement curves of different specimens

4. Finite Element Calculation

4.1. Material Model and Constitutive Relation

The model of ribbed square steel tube recycled concrete short column was created using the finite element program ABAQUS, and the short column's load-displacement relationship curve was simulated and studied. The steel constitutive model uses the isotropic elastic-plastic model, whereas the recycled concrete constitutive model uses the concrete plastic damage model in the material library.

4.2. Unit Type and Grid Division

Selecting the appropriate element is an important prerequisite for establishing a reasonable finite element model. ABAQUS provides a variety of element types for different materials in its finite element software. The model for the short column made of recycled concrete with a thin-walled ribbed square steel tube consists of two parts: the ribbed square steel tube and the core recycled concrete.

The meshing of element has an important influence on the convergence and convergence of the model's finite element. When the unit grid size is small, the model calculation takes a long time, but the simulation results are more accurate. When the unit grid size is large, the model calculation takes less time, but the simulation results' accuracy decreases. Therefore, selecting the appropriate mesh size can meet the requirements of convergence, calculation time and accuracy at the same time. In this article, we first choose a grid size of B/8 for the grid experiment, and then incrementally encrypt the grid with grid sizes of B/10, B/12, B/14, and B/16 until the difference between both findings is under one percent, at which point the grid density is regarded adequate. Considering the requirements of calculation accuracy and calculation time, this paper selects B/16 as the finite element model's mesh size, and all the concrete components are divided into hexahedral shapes, using structured mesh generation technology. The mesh division of the meta-model is shown in Figure 4.

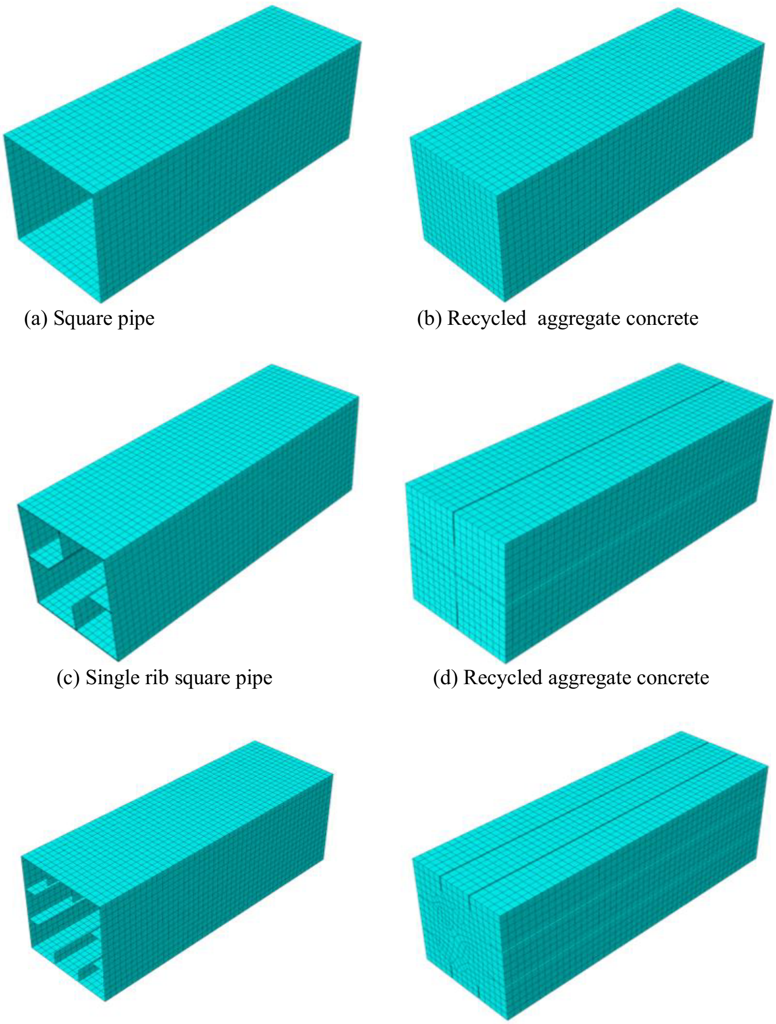

(a) Square pipe (b) Recycled aggregate concrete

(c) Single rib square pipe (d) Recycled aggregate concrete

(e) Double rib square pipe (f) Recycled aggregate concrete

Figure 4. Mesh generation of abaqus finite element model

4.3. Model Interface between Concrete and Steel Tubing

There are primarily three types of contacts in the finite element model in this chapter: stiffener and steel pipe, concrete andsteel pipe, stiffener and concrete. Together with the stiffening rib, the steel tube forms the ribbed square steel pipe, so it is combined together in the form of binding; the interface model between stiffener and recycled concrete and the interface model between steel tube and recycled concrete both adopt the action mode of surface-to-surface contact. The surface with large stiffness (steel tube and stiffener) is used as the main surface, and the surface with small stiffness (recycled concrete) is used as the secondary surface. The contact effect consists of both bond slide along the tangential direction and contact on the interface's normal direction.

The research results of Baltay and Gjelsvik[13] show that the coefficient of friction at the interface between concrete and low carbon steel typically ranges from 0.2 to 0.6.

When Schneider[14] and Hu[15] carried out the finite element analysis of concrete filled steel tube, the values of interfacial friction coefficient were 0.25 and 0.3 respectively. In this paper, the parametric study of the interface friction coefficient is carried out, and it is found that the different values have little effect in the curve of load displacement of the reused concrete packed steel pipe. When the interface friction coefficient is 0.25, the conclusions of the study of finite elements are nearer the data from the experiment, so the value of the interface friction coefficient is 0.25.

4.4. The Application of Loads and Boundary Conditions

First, reference points RP-1 and RP-2 are positioned 50 mm from the column's top and bottom, respectively. Then, the steel pipe and concrete at both ends of the short column are bound to the reference points as rigid bodies respectively. Finally, the reference point is subjected to the boundary conditions: RP-2 is totally fixed, whereas the top of the column (RP-1) only releases vertical degrees of freedom. The vertical degree of freedom U3 is set to 1, which is controlled by the amplitude and loaded by displacement.

4.5. Finite Element Analysis and Experimental Comparison

(1) Broken form Broken form. Figure 5 depicts a comparison of the SU-0-0 and SS-1-30 test modes of failure with the infinite element calculation. Figure 5 shows that the failure mode of the ribless specimen SU-0-0 simulated by ABAQUS is similar with the experimental phenomenon, with the largest buckling occurring in the center of the object in question. Due to the existence of stiffeners, there are two obvious half-waves in the transverse direction of the tube wall of the specimen SS-1-30, which is consistent with the experimental phenomenon. Because the experimental conditions are not completely consistent with the ideal simulation conditions, the deformation of the simulated members is inconsistent with that of the actual members in some areas. The specimen SU-0-0 has two large buckling in the longitudinal direction, while there is only one vertical section in the test. There is no half-wave in the upper part of the simulated specimen SS-1-30, because the model's boundary constraints set the two ends of the short column as rigid bodies and will not induce considerable deformation. But on the whole, the modes of failure of the specimen being simulated and the real-world specimen are consistent, which shows the correctness of the model.

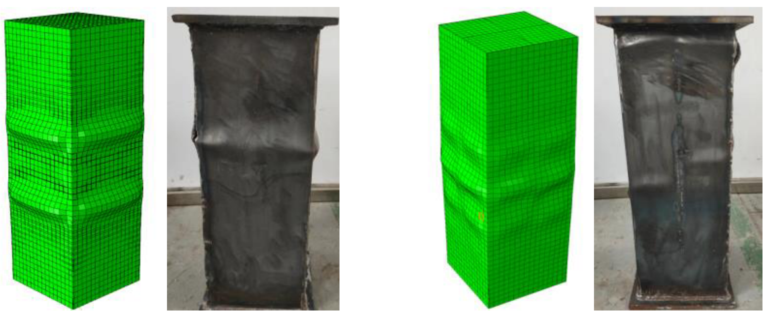

(a)SU-0-0 (b)SS-1-30

Figure 5. Comparison of failure patterns

(2) Load and displacement curve. Figure 6 shows actual load-displacement lines from the finite- elements simulation and the test data. The diagram illustrates that the model is able to simulate the peak load of the specimen and the descending part of the simulation curve in a better way. Table 1 compares the experimental value N_u with the ultimate bearing capacity N_0 determined by ABAQUS. N_u / N_0 has an average number of 0.975 and a standard error of 0.025.

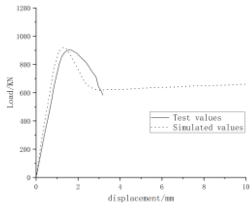

(a) SU-0-0

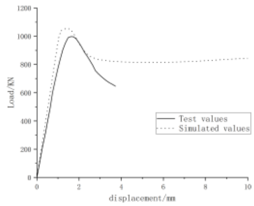

(b) SS-1-20

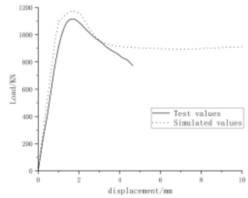

(c) SS-1-30

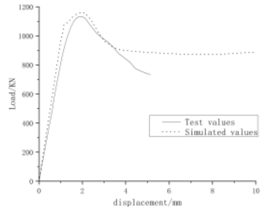

(d) SS-1-40

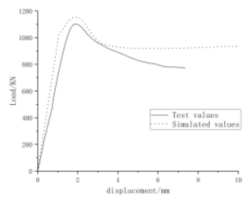

(e) SS-2-20

Figure 6. Comparison between load-displacement test curve and finite element curve

5. Conclusion

(1) Compared to the non-ribbed examples, the ribbed specimens had a substantially better carrying capacity. Stiffeners can be added to recycled concrete filled steel tube short columns to improve the restraint effect on the recycled concrete, postpone pipe wall buckling, and increase the short columns' ultimate bearing capacity. (2) When the specimen's width-to-thickness ratio is low, adding more stiffeners won't be able to significantly increase its bearing capacity; instead, it will cause the specimen's bearing capacity to be slightly lower. This is the case with the thin-walled, ribbed square steel tube recycled concrete short column. (3) The axial stiffness of the specimen is not much affected by increasing the stiffener's height-thickness ratio, but it can significantly increase the short column's ultimate bearing capacity, strengthen the constraint on the recycled concrete, and increase the specimen's ductility. (4) The finite element simulation's peak load has a maximum error of 5% compared to the test value. Additionally, the failure mode and load-displacement curve match the test results, indicating that the finite element software can well simulate the situation in the test, save costs and improve efficiency for subsequent research work.

The combined structure studied in this paper can be widely used in the new infrastructure of smart cities. Driven by the new infrastructure, it can not only realize the iterative upgrading of urban digitization, but also reduce the environmental pollution caused by abandoned buildings, which is conducive to building a sustainable smart city.

References

[1] Yin Di, Du Zhichao. Overview of the research status and application prospect of reclaimed concrete. Residence, 2022 (10): 39-41.

[2] Young R F, Lieberknecht K. From smart cities to wise cities: ecological wisdom as a basis for sustainable urban development. Journal of Environmental Planning and Management, 2019, 62(10): 1675-1692.

[3] Cole L B. Green building literacy: a framework for advancing green building education. International Journal of STEM Education, 2019, 6(1): 18.

[4] Spicer Z, Goodman N, Wolfe D A. How ‘smart’ are smart cities? Resident attitudes towards smart city design. Cities, 2023, 141: 104442.

[5] Nilssen M. To the smart city and beyond? Developing a typology of smart urban innovation. Technological Forecasting and Social Change, 2019, 142: 98-104.

[6] Manirathinam T, Narayanamoorthy S, Geetha S, et al. Assessing performance and satisfaction of micro-mobility in smart cities for sustainable clean energy transportation using novel APPRESAL method. Journal of Cleaner Production, 2024, 436: 140372.

[7] Kumar S, Gupta P K, Iqbal M A. Experimental and numerical study on self-compacting alkali-activated slag concrete-filled steel tubes. Journal of Constructional Steel Research, 2024, 214: 108453.

[8] GÜNeyisi E. Axial compressive strength of square and rectangular CFST columns using recycled aggregate concrete with low to high recycled aggregate replacement ratios. Construction and Building Materials, 2023, 367: 130319.

[9] Xiao Jianzhuang, Lei Bin, Yuan Biao. Study on the distribution characteristics of the compressive strength of reclaimed concrete from different sources. Journal of Architecture, 2008 (05): 94-100.

[10] Xiao Jianzhuang. Experimental study on uniaxial compressive stress and full strain curve of reclaimed concrete. Journal of Tongji University (Natural Science Edition), 2007 (11): 1445-1449.

[11] Wang Haiyang, Xiaoxiong, Huang Heshun, et al. Experimental study on the creep influence of steel pipe expansion and reclaimed concrete structure construction. Industrial buildings, 2011, 41 (06): 43-46.

[12] Huang Hong, Sun Wei, Chen Mengcheng, et al. Experimental study on mechanical properties of short column in square steel pipe. Journal of Architecture, 2015, 36 (S1): 215-221.

[13] Baltay P, Gjelsvik A. Coefficient of Friction for Steel on Concrete at High Normal Stress. Journal of Materials in Civil Engineering, 1990, 2(1): 46-49.

[14] Schneider S P. Axially Loaded Concrete-Filled Steel Tubes. Journal of Structural Engineering, 1998, 124(10): 1125-1138.

[15] Hu H, Huang C, Wu M, et al. Nonlinear Analysis of Axially Loaded Concrete-Filled Tube Columns with Confinement Effect. Journal of Structural Engineering, 2003, 129(10): 1322-1329.